Proton transfer reaction mass spectrometry investigations on the effects of reduced electric field and reagent ion internal energy on product ion branching ratios for a series of saturated alcohols

P. Brown[a], P. Watts[a], T.D. Märk[b], C.A. Mayhew[a],*

[a] School of Physics and Astronomy, University of Birmingham, Birmingham, B15 2TT, UK
[b] Institut für Ionenphysik und Angewandte Physik, Leopold Franzens Universität Innsbruck, Technikerstr. 25, A-6020 Innsbruck, Austria

ARTICLE INFO

ABSTRACT

In this paper we report an investigation of the effects of E/N over the range of 90–140 Td on the product ions resulting from the reactions of H_3O^+ with 12 saturated alcohols using a proton transfer reaction mass spectrometer (PTR-MS). The alcohols included in this study are methanol, ethanol, 1-propanol, 2-propanol, 1-butanol, 2-methyl-1-propanol, 2-methyl-2-propanol, 2-butanol, cyclopentanol, 1-pentanol, cyclohexanol, and 1-hexanol. Only in the cases of methanol and ethanol are any substantial amounts of the protonated parent observed at any E/N. For the other saturated alcohols predominantly fragment ions are observed. This implies that attempts to identify and hence monitor saturated alcohols in trace concentrations in a complex chemical environment using PTR-MS will be fraught with difficulties because a given m/z will not be unique to a particular chemical compound, i.e., multiple species could be present at a given m/z. In addition to changes in E/N we present preliminary results with regards to changing the conditions in the generation of the reagent ions via altering the operational conditions within the ion source (a hollow cathode). We present product ion branching ratios as a function of hollow cathode emission current for cyclohexanol, 1-propanol and 2-propanol at fixed E/N. Although not part of the reaction chamber, we have found that changing the hollow cathode emission current results in modifications to the product ion branching ratios. We presume that these observed changes are a result of altering the internal energies of the reagent ions and thereby modify the reaction kinetics and dynamics occurring within the drift tube of a PTR-MS.

© 2010 Elsevier B.V. All rights reserved.

1. Introduction

Following the extremely successful development [1] and commercialisation (Ionicon GmbH, Innsbruck, Austria) [2] of the proton transfer reaction mass spectrometer (PTR-MS) in the mid 1990s, there has been considerable growth and exploitation of proton transfer reaction mass spectrometry for trace gas monitoring in various chemical and physical environments [3–7], and in particular for the detection of volatile organic compounds (VOCs). Areas of application include atmospheric chemistry, environmental chemistry, plant and tree emissions, and food and medical sciences. A recent and comprehensive review by Blake et al. discusses in some detail all of these applications [8]. Proton transfer reaction mass spectrometry has rapidly become the preferred method for the monitoring of VOCs in many analytical areas and in particular where fast response times and high sensitivities are required. It is

these fast response times and high sensitivities which make PTR-MS such a useful and unique tool for monitoring VOCs in known atmospheres.

Given its growing use, it is important to not only highlight the considerable advantages of using PTR-MS as an analytical tool but also to research and discuss any properties of PTR-MS, which could be used to increase its already considerable potential.

In a complex chemical environment the identification of any VOCs present can be problematic, because without knowing what is in the sample the measurement of a given m/z cannot necessarily be assigned to a protonated parent or to a fragment ion, and could even be the result of multiple species that cannot be separated by a PTR-MS system without further advances in the technology. This aspect of PTR-MS was realised early on in the development of PTR-MS by Lindinger et al. [3] In their paper they state that "PTR-MS is a method for on-line monitoring and not primarily for gas analysis" and that GC–MS should be used for that purpose. An additional complication that arises with PTR-MS is the variation in product ion branching ratios caused by differences in operational variables, e.g., the choice of reduced electric field, and voltages on transmission optics, and/or

* Corresponding author. Tel.: +44 121 414 4729; fax: +44 121 414 4403.
 E-mail address: c.mayhew@bham.ac.uk (C.A. Mayhew).

by types of ionisation sources and operating conditions of those sources, which can make comparison of results between different studies troublesome.

Objectives of this paper are to illustrate the difficulties that can arise with the identification of chemical compounds using PTR-MS and to show how some of the operational parameters that can affect the outcome of measurements (product ion branching ratios), using saturated alcohols as the chemical compounds of interest. The series of saturated alcohols used in this study cover a range of molecular weights and structures, namely (and in order of increasing molecular weight); methanol (CH_3OH), ethanol (C_2H_5OH), 1-propanol ($CH_3CH_2CH_2OH$), 2-propanol ($CH_3CHOHCH_3$,), 1-butanol ($CH_3CH_2CH_2CH_2OH$), 2-methyl-1-propanol ($CH_3(CH_2)_3OH$), 2-methyl-2-propanol(($CH_3)_3COH$), 2-butanol ($CH_3CH(OH)CH_2CH_3$), cyclopentanol (C_5H_9OH), 1-pentanol ($C_5H_{11}OH$), cyclohexanol ($C_6H_{11}OH$), and 1-hexanol ($CH_3(CH_2)_5OH$).

2. Proton transfer reaction mass spectrometry

At the heart of its operation is a reaction region consisting of a drift tube into which the gas (air) sample to be analysed is introduced. The use of this instrument therefore requires an operational choice to be made by the user for the ratio of the electric field strength (E) – the voltage gradient down the drift tube – to the buffer gas number density (N) (i.e., the pressure within the drift tube) for a particular application. The choice of reduced electric field strength, E/N, affects the reaction dynamics occurring within the drift tube because it alters the primary reagent ion signal, i.e., particularly the ratio of intensities of the H_3O^+ to $H_3O^+ \cdot (H_2O)_n$ ($n \geq 1$) signals, the reaction time (drift time), the reagent ion-neutral collisional energy and the collisional induced dissociation of the product ion(s) leading to their fragmentation. Hence differences in product ion branching ratios may be observed which result either from an E/N dependence and/or the differences in the reaction kinetics and dynamics of the protonated water monomers and protonated water clusters with VOCs or both. Altogether these make any mechanistic interpretations of PTR-MS data extremely difficult.

In addition to the E/N dependence mentioned above, the distribution of the $H_3O^+ \cdot (H_2O)_n$ ($n \geq 0$) reagent ions in the drift tube is dependent also on the humidity in and temperature of the drift tube. At high E/N (defined here to be greater than approximately 120 Td (1 Td = 10^{-21} V m^2)) cluster ion formation is significantly reduced such that even for humid air samples the sum of the protonated water ion clusters usually accounts for less than approximately 20% of the total reagent ion intensity in the drift tube. This is substantially less when "dry air" is introduced into the drift tube. Fig. 1(a) shows the relative cluster ion concentrations for the protonated water monomer, dimer and trimer when dry nitrogen (15 ppmv of water (measured using an EASIDEW portable hygrometer)) is introduced into the drift tube of an Ionicon PTR-MS Quadrupole system as the buffer gas. Note that although the nitrogen introduced is dry, water vapour from the hollow cathode of the PTR-MS will diffuse into the drift tube [9]. As can be seen from Fig. 1(a) the cluster reagent ions (and in particular the protonated water dimer at m/z 37) intensities increase as E/N is reduced, and become the dominant reactive species in the drift tube below about 95 Td. The protonated water cluster ion intensities have increased at the expense of the protonated water monomer intensity. This is because the collisional dissociation energy available has decreased reducing the fragmentation of the protonated water cluster ions and the reactant time has increased. It should be noted that there is some question whether these signal intensities recorded provide an accurate representation of the distribution of the protonated water clusters in the drift tube. It is possible that the measured distribution is distorted either by collisional processes or additional
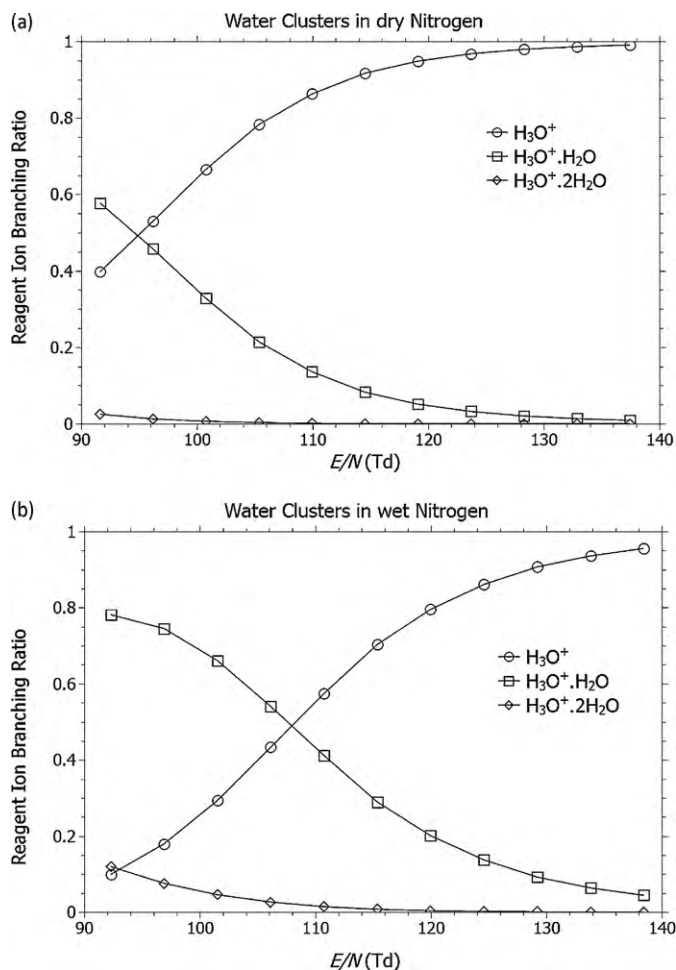
Fig. 1. Relative reagent ion branching ratios for the distribution of H_3O^+, $H_3O^+ \cdot H_2O$ and $H_3O^+ \cdot (H_2O)_2$ detected using a PTR-MS with the drift tube maintained at 2.060 ± 0.005 mbar and 312 ± 2 K as a function of reduced electric field strength (E/N) for (a) dry nitrogen filtered through a molecular sieve and (b) dry nitrogen filtered through a molecular sieve and then bubbled through a Dreschel bottle containing highly purified water. Note that the signal intensity of H_3O^+ is too large to be measured directly using the PTR-MS. Therefore, the signal intensity at $m/z = 21$ corresponding to $H_3{}^{18}O^+$ was recorded for both the data presented in both (a) and (b). The $m/z = 19$ intensity was determined in the normal manner by multiplying the $m/z = 21$ signal by 487. Similarly for measurements below $E/N = 110$ Td for (a) and for all E/N for (b), the $m/z = 37$ signal was not measured directly owing to its high intensity. Instead its oxygen 18 isotope at $m/z = 39$ ($H_3{}^{18}O^+ \cdot H_2O$ or $H_3O^+ \cdot H_2{}^{18}O$) was used for the measurements.

clustering in the expansion region between the drift cell and the mass spectrometer. However, given the changes in the reagent ion concentrations as a function of E/N it is considered that this is a small effect. That the humidity within the drift tube has a significant role to play in determining at which E/N the water cluster ions become the dominant species is illustrated in Fig. 1(b). The data shown in this figure were recorded after bubbling nitrogen gas through water contained in a Drechsel bottle, and hence the N_2 buffer gas is classified as being "wet" – being close to 100% saturation. The changes in the relative intensities of the water cluster ions compared to the protonated water monomer for these two conditions are obvious when comparing Fig. 1(a) and (b). This is a significant observation because proton transfer reactions involving the water cluster ions to a VOC are less energetic than those involving the protonated water monomer. Thus, for example, an increase in the protonated water cluster ion intensity may lead to less dissociative proton transfer. When proton transfer is endothermic protonated water cluster ions may react with a VOC through a mechanism that leads to the $MH^+ \cdot H_2O$ product ions, and then

through collisions (either in the drift tube or in the interface region between the drift tube and the low pressure environment of the mass spectrometer) $MH^+ \cdot H_2O^+$ may fragment to $MH^+ + H_2O$. Such processes must be taken into account when analysing PTR-MS data. Despite the clear dependence of product ion branching ratios on E/N (and hence the mean collisional energy between reagent ions and neutrals) and humidity, these quantities are sometimes overlooked in PTR-MS studies.

With reference to the ion temperature, it is important to mention that in addition to E/N dependences, the internal energy distribution of the protonated water molecules (and protonated water clusters) should also be considered, because the energy in the proton transfer reaction will be dependent on the available energy, which in turn will depend on the internal energy available. In the ionisation source the H_3O^+ ions will presumably be produced with a spread of internal energies which may be non-thermal, and which may depend on the type of ionisation (radioactive, microwave, or electrical discharge) and operating conditions. This raises the question as to how efficient are the collisions of these reagent ions with the (air) buffer gas in the drift tube to thermalise the reagent ions' internal energy distribution. Therefore an additional parameter to explore is the type of ionising source to produce the reagent ions and the operating conditions of that source. By varying these conditions, e.g., for an electrical discharge in a hollow cathode source the current and accelerating lenses, it should be possible to alter the internal energy distribution of the H_3O^+ swarm in the drift tube and thereby affect the kinetics and dynamics of the ion-molecule reactions occurring within the drift tube.

Towards the above goals we have instigated a series of studies involving various families of VOCs in which E/N and the operating condition of the hollow cathode are altered to investigate their effects on the product ion branching ratios. In this paper we concentrate predominantly on a detailed investigation of the effects of E/N on the product ion branching ratios to a series of saturated alcohols. For a subset of the alcohols we have also investigated the effects of hollow cathode emission current on the product ion distributions for fixed E/N.

The saturated alcohols have been specifically chosen for this study because non-dissociative proton transfer is not a dominant channel, and predominantly fragment ions are observed. Similar systematic E/N studies have been undertaken investigating dependences of the product ion distributions with various VOCs by various other groups [10–14], and in particular we note that in the preparation of this paper a related study to ours but involving unsaturated alcohols has been recently published [14]. To our knowledge there have been no previous PTR-MS studies which discuss the potential effect of reagent ion internal energy on product ion distributions.

3. Experimental details

The PTR-MS used in this study is an analytical quadrupole mass spectrometric instrument specifically designed and built by Ionicon Analytik GmbH to monitor low concentrations (of the order of parts per trillion by volume) of VOCs present in a chemical environment in real-time. PTR-MS has been described in detail in the literature [1–8] and hence only a brief description of the apparatus will be provided.

A high-density constant current of reagent ions is provided by means of a hollow cathode ion source operated with water vapour. The operating emission current for the hollow cathode can be varied from 1 to 10 mA, but for the majority of the measurements the hollow cathode was run at a value of 5 mA. Only for the measurements presented in the last part of the results section of this paper was the hollow cathode emission current varied. The ions that are produced within the hollow cathode discharge undergo a series of
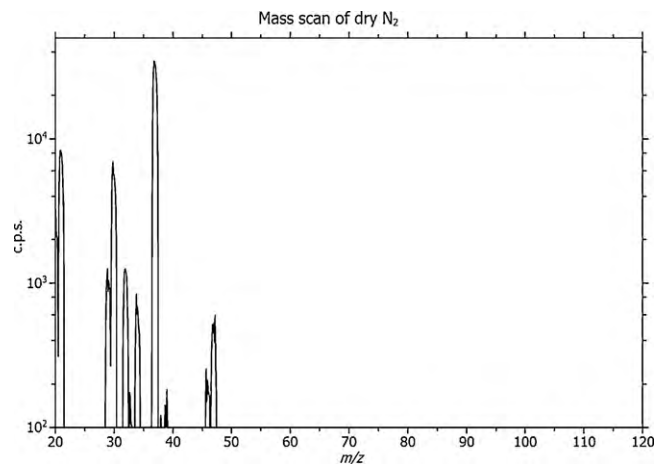

Fig. 2. Background mass spectrum recorded using the PTR-MS over an m/z range of 20–120 amu at an E/N of 140 Td and hollow cathode current of 5 mA for dry nitrogen before any ROHs are introduced into the drift tube. A number of peaks are observed either as a result of being produced in the ionisation source or as a result of reactions in the drift cell with trace impurities. The m/z values (assigned ion) are m/z 21 ($H_3^{18}O^+$), 29 (fragment from protonated ethanol and N_2H^+), 30 (NO^+), 32 (O_2^+), 37 ($H_3O^+ \cdot H_2O$), 46 (NO_2^+), and 47 ($C_2H_5OH_2^+$ (protonated ethanol) or $CH_2O_2H^+$ (protonated formic acid)).

ion-molecule reactions ultimately resulting in reagent ions mainly associated with protonated water or protonated water clusters. However, other ions such as O_2^+ and NO^+ are still present in the ion swarm within the drift tube, but usually at less than 2% of the total ion intensity. All of these ions are transported into a drift-tube containing the gas sample (e.g., ambient air) through which they drift under the action of an electric field. A fraction of these ions are sampled through an orifice at the end of the drift tube, analysed by a quadrupole mass spectrometer and detected by a secondary electron multiplier. Fig. 2 shows a typical mass spectrum obtained for a dry nitrogen sample after it has passed through a molecular sieve (an ALL-Pure hydrocarbon trap, which removes hydrocarbons to <3 ppb) and before any VOCs are introduced into the drift tube of the PTR-MS. Upon introduction of VOCs, reagent ion-VOC reactions occur in the drift tube and the product ions can be monitored in the same way as for the reagent ions.

In this study we have kept N constant by maintaining the pressure and temperature of the drift tube at 2.060 ± 0.005 mbar and 312 ± 2 K, respectively, whilst varying the voltage across the drift tube over the range available on the Ionicon PTR-MS, namely 400–600 V. This leads to values of E/N over the range of approximately 90–140 Td.

Saturated alcohol (ROH) samples were introduced into the PTR-MS by the use of a syringe and syringe drive (used to vary the concentration entering the drift tube of a PTR-MS in a reproducible manner). A drop of a ROH was placed onto cotton wool, which had been placed inside the syringe. The syringe was filled with commercial grade N_2 previously passed through a hydrocarbon trap and then inserted into a septum connected to a 1/8 in. Teflon pipe through which N_2 was flowing. The N_2 line was connected to the inlet of the PTR-MS using a Swagelok T-piece so that the N_2 and any ROH in the line could be sampled through a needle valve into the drift tube of the PTR-MS. Therefore we are determining the branching ratios of the product ions as measured in a "dry" buffer gas in order to reduce humidity effects. The majority of the N_2 and any trace ROH were then exhausted to the atmosphere outside of the laboratory. Teflon tubing was used in this study for the inlets in order to minimize memory effects on surfaces [9,15].

All of the saturated alcohols used in this study were purchased from Sigma–Aldrich (purities $\geq$ 99%) and all were used without any further purification.
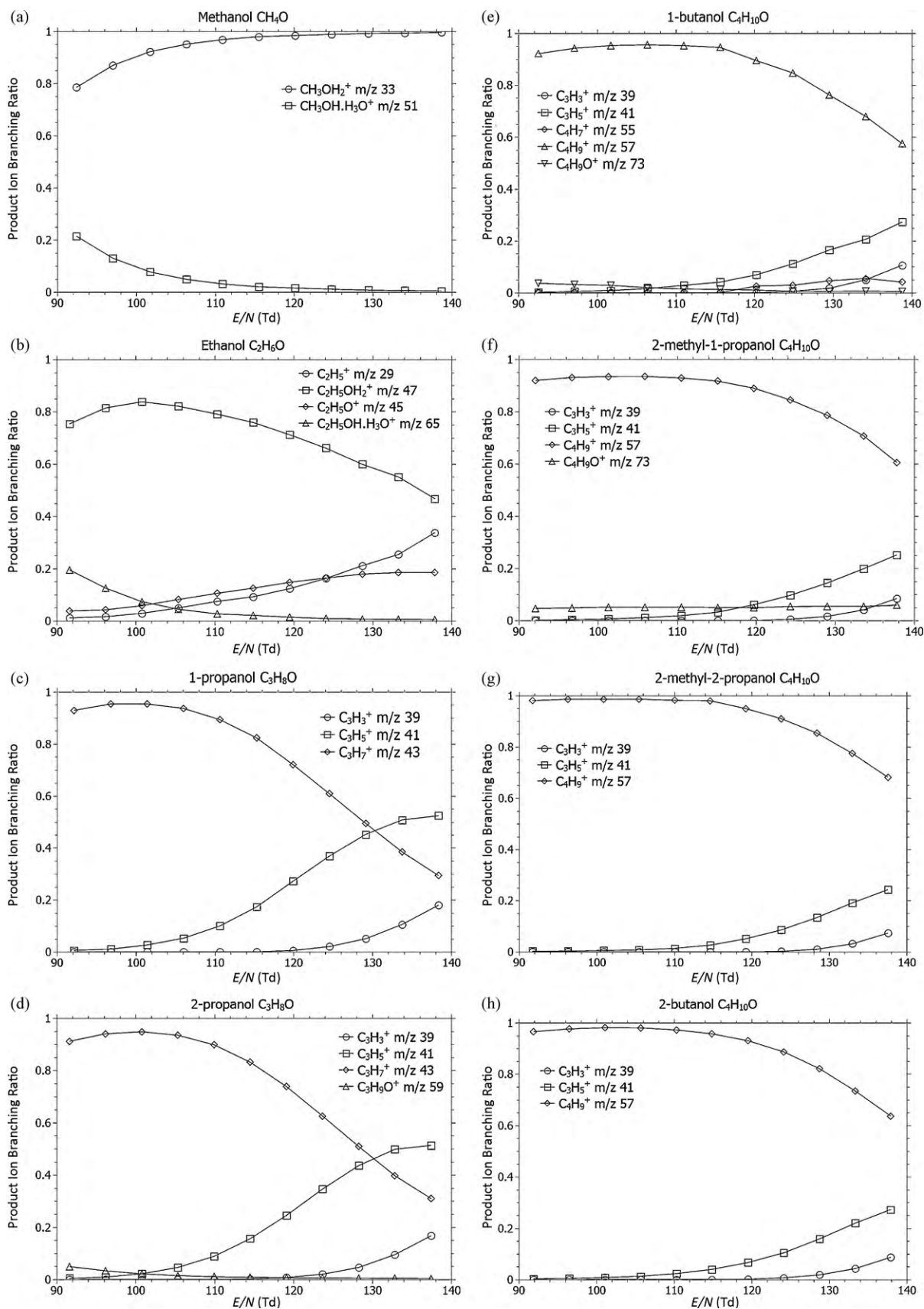
Fig. 3. Product ion distributions (branching ratios) as a function of E/N for (a) methanol, (b) ethanol, (c) 1-propanol, (d) 2-propanol, (e) 1-butanol, (f) 2-methyl-1-propanol, (g) 2-methyl-2-propanol, (h) 2-butanol, (i) cyclopentanol, (j) 1-pentanol, (k) cyclohexanol, and (l) 1-hexanol. Note for clarity only those product ions with branching ratios of greater than 1% are provided on these figures although the ions with 1% intensity are provided in Table 1. Note that the hollow cathode current for all of these measurements was maintained at 5 mA.
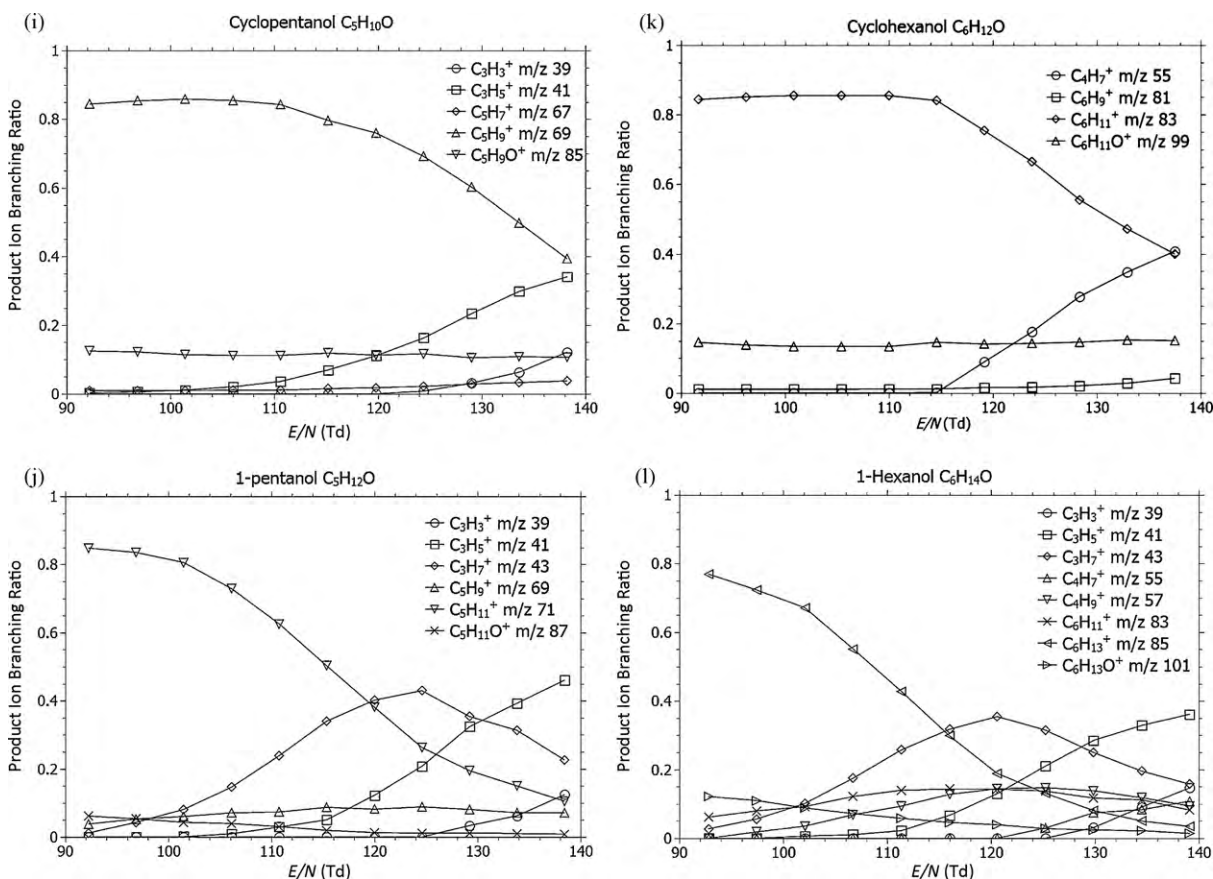
Fig. 3. (*Continued*).

4. Results

The presentation and discussion of the results are divided into two sections. Section 4.1 deals with the product ion branching ratios of all of the saturated alcohols investigated for this study as a function of E/N whilst operating the hollow cathode at an emission current of 5 mA (the manufacturer's recommended value). Section 4.2 shows for the first time the effects of the hollow cathode emission current on the product ion branching ratios at fixed E/N values for three of the saturated alcohols, namely cyclohexanol, 1-propanol and 2-propanol.

4.1. E/N dependencies with a fixed hollow cathode emission current of 5 mA

The fragmentation patterns for the alcohols as a function of E/N are shown in Fig. 3(a)–(l) and summarized in Table 1 for three values of E/N of 92, 115 and 138 Td (typical operating value for PTR-MS studies are 120–140 Td). None of the alcohols, with the exceptions of methanol and ethanol produces other than trace amounts of the protonated alcohol, ROH_2^+, thus negating one of the usefulnesses of PTR-MS that gentle protonation generally produces the protonated parent thus aiding identification, at least to the extent that the mass of the parent can be determined. All of the alcohols, with the exception of methanol, show a fragmentation pattern that is dependent upon E/N and the complexity of which increases with the size of the alcohol. A contributing factor to this complex behaviour is that in addition to primary fragmentation, secondary fragmentation also occurs and thus the apparent branching ratio will change as the reaction time changes.

It was stated earlier that the PTR-MS could not produce data on fragmentation patterns that could be easily analysed in terms of kinetics and mechanisms as the single controllable experimen-

tal variable, E/N, changes several parameters, viz. the energy of the reactant ions, the energy of the product ions, and the drift and thus the reaction times of the various ions. Although this is true, there is a wealth of information on ion-neutral reactions and ion fragmentations in the data presented in this paper and it would be remiss if it were to be ignored. A brief discussion of mechanisms suggested by the present data will be given although a fuller analysis awaits the completion of DFT calculations and incorporation of SIFT, ESI-ITMS and IMS-MS data on related compounds.

4.1.1. Methanol

Methanol, which is a ubiquitous compound in the atmosphere and is the simplest alcohol, has been studied by several groups using PTR-MS [16,17]. For any E/N used, the only product ion observed by these other studies is the protonated parent at m/z 33. Our results shown in Fig. 3(a) are in agreement with these earlier measurements over most of the E/N range investigated. Only at low E/N did we observe an additional product ion associated with the clustering of the protonated methanol monomer species to H_2O to produce $ROH_2^+ \cdot H_2O$.

4.1.2. Ethanol

The behaviour of the proton transfer reaction from H_3O^+ to ethanol in a PTR-MS has been described in the literature as anomalous owing to major differences in product ion branching ratios [18]. This anomaly is however readily explainable. The proton transfer reaction to ethanol is unique amongst the saturated alcohols in that, providing the energy of the reaction is sufficient, m/z 19 (H_3O^+) is also produced from ROH_2^+ and, owing to its energy dependence, its associated branching ratio is very much dependent on the value of E/N used in PTR-MS measurements. This highlights again the importance of specifying E/N for any PTR-MS measurements.

Table 1

Product ions identified and their associated product ion branching ratios (percentage in parentheses) measured at E/N values of 92, 115 and 138 Td for a series of saturated alcohols (ROH) presented firstly in order of increasing molecular weight. For these measurements the ROHs were separately injected in trace quantities into a flow of dry nitrogen that was sampled into the drift tube of the PTR-MS. Slight differences of the product ion branching ratios to those presented in Fig. 3 are a result of the branching ratios in the table being extrapolated to zero concentration to allow for any secondary ion-molecule processes. The hollow cathode was maintained at an operational current of 5 mA. Errors in the branching ratios are estimated to be less than 10%.

Chemical name	Molecular formula (MW)	Product ions and ion branching ratios (%)		
		$E/N = 92$ Td	$E/N = 115$ Td	$E/N = 138$ Td
Methanol	CH_3OH (32)	51 (21) $ROH \cdot H_3O^+$ 33 (79) ROH_2^+	51 (2) $ROH \cdot H_3O^+$ 33 (98) ROH_2^+	33 (100) ROH_2^+
Ethanol[a]	C_2H_5OH (46)	19 (?) H_3O^+ 65 (20) $ROH \cdot H_3O^+$ 47 (75) ROH_2^+ 45 (4) $[ROH-H_2]H^+$ 29 (1) R^+	19 (?) H_3O^+ 65 (1) $ROH \cdot H_3O^+$ 47 (69) ROH_2^+ 45 (15) $[ROH-H_2]H^+$ 29 (15) R^+	19 (?) H_3O^+ 47 (43) ROH_2^+ 45 (17) $[ROH-H_2]H^+$ 29 (40) R^+
1-Propanol	C_3H_7OH (60)	79 (4) $ROH \cdot H_3O^+$ 61 (3) ROH_2^+ 43 (93) R^+	43 (83) R^+ 41 (17) $[R-H_2]^+$	43 (29) R^+ 41 (52) $[R-H_2]^+$ 39 (19) $[R-2H_2]^+$
2-Propanol	C_3H_7OH (60)	79 (3) $ROH \cdot H_3O^+$ 61 (5) ROH_2^+ 59 (1) $[ROH-H_2]H^+$ 43 (91) R^+	59 (1) $[ROH-H_2]H^+$ 43 (85) R^+ 41 (14) $[R-H_2]^+$	59 (1) $[ROH-H_2]H^+$ 43 (31) R^+ 41 (52) $[R-H_2]^+$ 39 (16) $[R-2H_2]^+$
1-Butanol	C_4H_9OH (74)	93 (3) $ROH \cdot H_3O^+$ 75 (1) ROH_2^+ 73 (5) $[ROH-H_2]H^+$ 57 (91) R^+	73 (2) $[ROH-H_2]H^+$ 57 (95) R^+ 41 (3) $[R-CH_4]^+$	57 (55) R^+ 55 (7) $[R-H_2]^+$ 41 (26) $[R-CH_4]^+$ 39 (12) $[R-CH_4-H_2]^+$
2-Methyl-1-propanol	C_4H_9OH (74)	93 (3) $ROH \cdot H_3O+$ 73 (5) $[ROH-H_2]H^+$ 57 (92) R^+	73 (7) $[ROH-H_2]H^+$ 57 (90) R^+ 41 (3) $[R-CH_4]^+$	73 (8) $[ROH-H_2]H^+$ 57 (58) R^+ 41 (26) $[R-CH_4]^+$ 39 (8) $[R-CH_4-H_2]^+$
2-Methyl-2-propanol	C_4H_9OH (74)	93 (1) $ROH \cdot H_3O^+$ 75 (1) ROH_2^+ 57 (98) R^+	57 (98) R^+ 41 (2) $[R-CH_4]^+$	57 (68) R^+ 41 (24) $[R-CH_4]^+$ 39 (8) $[R-CH_4-H_2]^+$
2-Butanol	C_4H_9OH (74)	93 (2) $ROH \cdot H_3O^+$ 75 (1) ROH_2^+ 57 (97) R^+	57 (96) R^+ 41 (4) $[R-CH_4]^+$	57 (63) R^+ 41 (28) $[R-CH_4]^+$ 39 (9) $[R-CH_4-H_2]^+$
Cyclopentanol	$C_5H_{10}O$ (86)	105 (3) $ROH \cdot H_3O^+$ 85 (16) $[ROH-H_2]H^+$ 69 (80) R^+ 67 (1) $[R-H_2]^+$	85 (17) $[ROH-H_2]H^+$ 69 (78) R^+ 67 (1) $[R-H_2]^+$ 41 (4) $[R-C_2H_4]^+$	85 (15) $[ROH-H_2]H^+$ 69 (35) R^+ 67 (5) $[R-H_2]^+$ 41 (32) $[R-C_2H_4]^+$ 39 (13) $[R-C_2H_4-H_2]^+$
1-Pentanol	$C_5H_{11}OH$ (88)	107 (3) $ROH \cdot H_3O^+$ 87 (10) $[ROH-H_2]H^+$ 71 (80) R^+ 69 (6) $[R-H_2]^+$ 43 (1) $[R-C_2H_4]^+$	87 (4) $[ROH-H_2]H^+$ 71 (49) R^+ 69 (12) $[R-H_2]^+$ 43 (30) $[R-C_2H_4]^+$ 41 (5) $[R-C_2H_4-H_2]^+$	71 (9) R^+ 69 (16) $[R-H_2]^+$ 43 (17) $[R-C_2H_4]^+$ 41 (44) $[R-C_2H_4-H_2]^+$ 39 (14) $[R-C_2H_4-2H_2]^+$
Cyclohexanol	$C_6H_{12}O$ (100)	119 (2) $ROH \cdot H_3O^+$ 99 (26) $[ROH-H_2]H^+$ 83 (71) R^+ 81 (1) $[R-H_2]^+$	99 (27) $[ROH-H_2]H^+$ 83 (71) R^+ 55 (1) $[R-C_2H_4]^+$ 81 (1) $[R-H_2]^+$	99 (27) $[ROH-H_2]H^+$ 83 (31) R^+ 55 (36) $[R-C_2H_4]^+$ 81 (6) $[R-H_2]^+$
1-Hexanol	$C_6H_{13}OH$ (102)	121 (1) $ROH \cdot H_3O^+$ 101 (20) $[ROH-H_2]H^+$ 85 (71) R^+ 83 (7) $[R-H_2]^+$ 43 (1) $[R-C_3H_6]^+$	101 (7) $[ROH-H_2]H^+$ 85 (19) R^+ 83 (21) $[R-H_2]^+$ 57 (16) $[R-C_2H_4]^+$ 43 (32) $[R-C_3H_6]^+$ 41 (5) $[R-C_3-H_2]^+$	101 (2) $[ROH-H_2]H^+$ 85 (1) R^+ 83 (12) $[R-H_2]^+$ 57 (10) $[R-C_2H_4]^+$ 55 (12) $[R-C_2H_4-H_2]^+$ 43 (12) $[R-C_3H_6]^+$ 41 (35) $[R-C_3H_6-H_2]^+$ 39 (16) $[R-C_3H_6-2H_2]^+$

[a] The product ion branching ratios for ethanol do not take into account the production of the product ion H_3O^+.

We are unable to allow for the production of H_3O^+, and therefore the product ion branching ratios presented in Fig. 3(b) and Table 1 do not take this into account. Fragment ions are observed at m/z 45 ($C_2H_5O^+$) corresponding to a loss of H_2, and m/z 29 ($C_2H_5^+$) corresponding to a loss of H_2O from the protonated species. At low E/N (approximately 90 Td) the protonated ethanol is observed to cluster forming $ROH_2^+ \cdot H_2O$ at m/z 65. In the PTR-MS work by Inomata and Tanimoto, in which isotopic labeling was used so that the m/z 19 channel could be taken into account when determining the product ion branching ratios, it should be noted that the product

ion at m/z 45 is not reported [19]. They report a product ion at m/z 31 assigned to be CH_2OH^+ which we did not observe. In agreement with our observations Buhr et al. did not observe a m/z 31 ion but do report the observation of the m/z 45 ion (which to our knowledge is the only other study dealing with the reactions of H_3O^+ with ethanol that has reported this channel) [16].

4.1.3. 1-Propanol and 2-propanol

These show very similar behaviour with the exceptions that at low E/N a trace of the protonated alcohol is observed for 2-propanol

but not 1-propanol. Also a trace of the ion, $C_3H_7O^+$, corresponding to formal loss of H_2 from the protonated alcohol, is observed for 2-propanol but not from 1-propanol (except when operating the hollow cathode ion source at higher emission currents, which will be discussed later). As the dominant reaction is loss of water from the protonated alcohol it is to be expected that the primary carbocation formed from 1-propanol will isomerise to the secondary propyl carbocation and thus subsequent fragmentation of sequential loss of H_2, $C_3H_7^+ \rightarrow C_3H_5^+ \rightarrow C_3H_3^+$ will be identical for the two alcohols. That this is so indicates that the isomerisation is rapid.

In their PTR-MS studies Buhr et al. report product ion branching ratios for 1-propanol and 2-propanol which are different from ours with the R^+ (corresponding to loss of H_2O from the protonated species) channel being reported as the dominant species with a branching ratio of approximately 70% and the $[R-H_2]^+$ channel (loss of H_2O and H_2 from the protonated species) at approximately 30% [16]. No m/z 39 ion (loss of H_2O and $2H_2$ from the protonated species) is reported by them. This could be a result of Buhr et al. using a lower E/N in their study. However, Buhr et al. only report that they operated the drift tube at a voltage of 600 V. To obtain their branching ratios we would need to operate our PTR-MS at an E/N of approximately 120 Td, which if we assume Buhr et al. were operating their system at room temperature places their drift tube pressure at approximately 2.25 mbar. This highlights once more the need to specify the operating conditions used in PTR-MS studies for comparisons to be made. Also in contrast to our measurements, Lindinger et al., using an E/N in the drift tube of 120–140 Td, observed a substantial branching ratio associated with

ion could also be formed by loss of H_2 from $C_4H_9^+$ but as it is not seen in the reactions of the other butanols it is concluded that this pathway does not occur. It is therefore concluded that the two ions with the empirical formula $C_4H_9O^+$ have different structures. For all alcohols the dominant ion is a butyl carbocation. As the subsequent fragmentation of this is identical for all the butanols it is concluded that isomerisation to the t-butyl carbocation is rapid. As stated above, t-$C_4H_9^+$ does not lose H_2 but loses CH_4 to give $C_3H_5^+$, which, as was seen in the reactions of the propanols, loses H_2 to give $C_3H_3^+$. It is an indication of the excess energy available in the drift cell of the PTR-MS that for the reaction of 2-methyl-2-propanol with H_3O^+ in both the atmospheric pressure IMS [20] and low pressure FTMS [21] no fragmentation of the t-butyl carbocation is observed.

In agreement with our observations, Buhr et al. also found that for 1-butanol, 2-methyl-2-propanol and 2-butanol the m/z 57 ion is the dominant species from the proton transfer reaction [16]. However, as found for the propanols, the product ion branching ratios are only in good agreement if Buhr et al. operated their PTR-MS at 120 Td. This would explain why Buhr et al. make no mention of the m/z 39 ion channel. Buhr et al. mention a fragment ion at m/z 58 which, given its relative intensity, we have taken to be the ^{13}C isotope of the m/z 57 ion.

4.1.5. 1-Pentanol and 1-hexanol

Fragmentation of these two primary alcohols is at first sight too complex to analyse. However plausible reaction schemes can be obtained by building upon the fragmentation patterns obtained from the smaller alcohols. These are
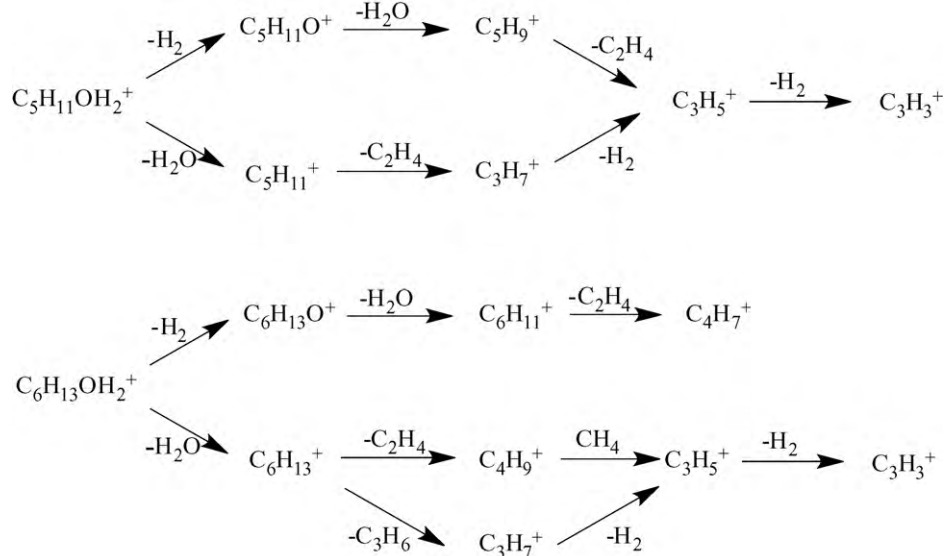
the protonated parent (20% for 1-propanol and 10% for 2-propanol), although (and in agreement with our findings) the dominant fragment is still m/z 43 (80% for 1-propanol and 90% for 2-propanol) [3]. The observation of substantial intensities associated with the protonated parents by Lindinger et al. at the E/N values they used implies that in comparison to our operating conditions either the proton transfer reaction is gentler and/or that their transfer optics led to less fragmentation.

4.1.4. The butanols

Only for the two primary alcohols 1-butanol and 2-methyl-1-propanol are traces of the ion, $C_4H_9O^+$, corresponding to formal loss of H_2 from the protonated alcohol observed. Loss of H_2 from protonated 2-methyl-1-propanol gives a stable ion but that from 1-butanol can lose water to give an ion with the empirical formula $C_4H_7^+$, but this is only observed at the higher values of E/N. This

For both alcohols the facile sequential loss of H_2 from $C_3H_7^+$ has been seen with both the propanols and butanols. Also the loss of CH_4 was seen from t-$C_4H_9^+$. The loss of H_2 followed by the loss of H_2O was seen with 1-butanol. Thus only the fragmentations of the C_5 and C_6 carbocations are new. It is interesting that the $C_4H_7^+$ carbocation from 1-hexanol appears stable as did the corresponding ion from 1-butanol. It is also interesting that the generic structure of the ion formed by sequential loss of H_2 and then H_2O from a straight chain primary alcohol only fragments by losing C_2H_4.

1-Pentanol and 1-hexanol have also been investigated by Buhr et al. [16]. Their 1-pentanol results bear no resemblance to our measurements. Of the fragment ions they observed; m/z 57 (90%), 41 (6%) and 58 (4%), we only observed m/z 41. Buhr et al.'s results for 1-hexanol are in better agreement with our measurements in that a larger number of product ions with the same m/z are observed in the two studies with similar product ion branching ratios

(assuming Buhr et al. operated the drift tube of their PTR-MS at 120 Td).

4.1.6. Cyclopentanol and cyclohexanol

The fragmentations of the carbocations formed following loss of water from the protonated alcohols mirror those observed for the corresponding straight chain primary alcohols and are shown below.
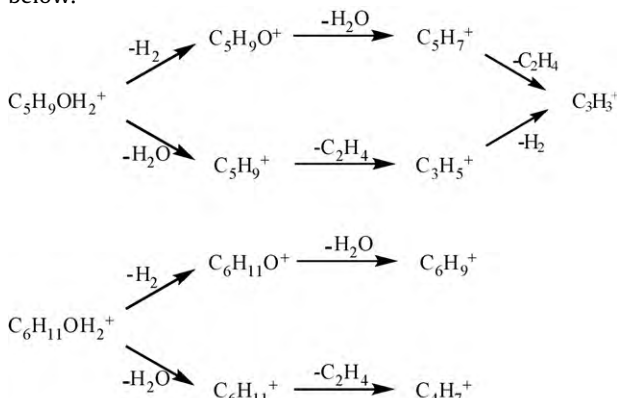

The facile loss of H_2 from the protonated cyclic alcohols is followed by subsequent fragmentation via loss of H_2O as is seen with the straight chain primary alcohols. The reaction of cyclohexanol with H_3O^+ has been reported in an IMS [22] and whilst loss of H_2 occurred no carbocation or fragmentation was observed.

4.2. The effects of the hollow cathode emission current on the product ion branching ratios for cyclohexanol, 1-propanol and 2-propanol

In this paper we have so far predominantly focused our attention on the effects of E/N on product ion branching ratios using saturated alcohols as sample compounds whilst keeping the hollow cathode emission current set at Ionicon's recommended level of 5 mA. However, as mentioned earlier the values of the product ion branching ratios will also be altered by parameters and conditions such as humidity, focussing lens voltages, and the "internal temperature" of the reagent ions exiting the ion source. Whilst some preliminary studies have investigated the effects of humidity and various lens voltages (which can be adjusted to reduce collisional induced dissociation in the low pressure environment after the drift tube) [7,9], to our knowledge there is no mention in the literature regarding the internal energy distribution of the reagent H_3O^+ ions. Here we make some comments on this.

The internal temperature of the reagent ion needs to be taken into consideration in its reaction with a ROH. Whilst this needs to be the subject of a detailed study, by way of examples here, in Fig. 4 we present the product ion branching ratios obtained for (a) cyclohexanol, (b) 1-propanol and (c) 2-propanol as a function of
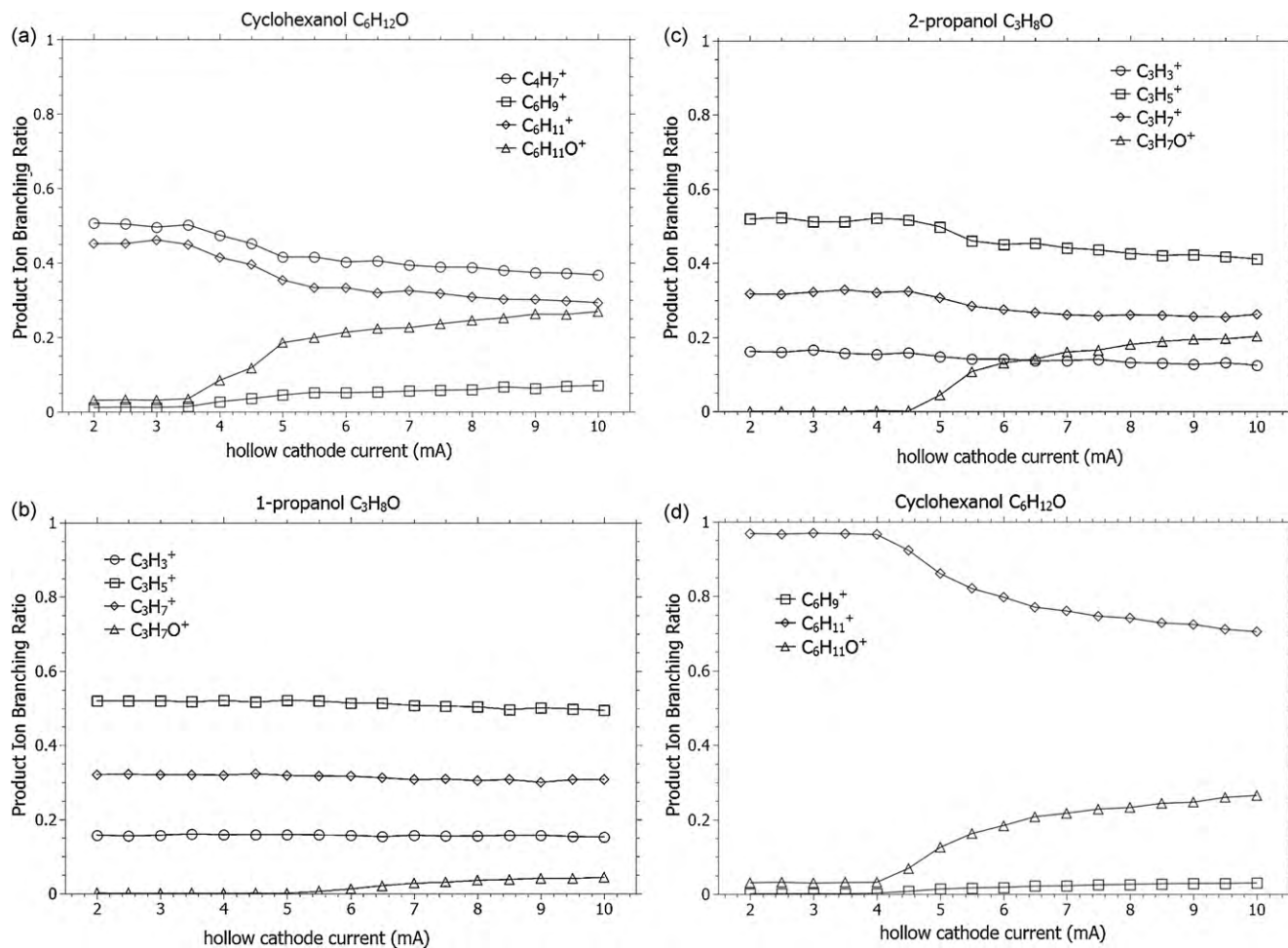
Fig. 4. Effects of hollow cathode emission current on the ion branching ratios of the product ions observed for the reaction of H_3O^+ with (a) cyclohexanol, (b) 1-propanol and (c) 2-propanol with the PTR-MS drift tube operating at 138 Td. (d) Repeats the measurements for cyclohexanol but at an E/N of 92 Td. For all these measurements the concentration of the respective saturated alcohol was kept constant. Note these measurements were not taken at the same time as the measurements made for Fig. 3 and so the state of the hollow cathode (i.e., cleanliness) would have changed (which in itself will modify the product ion branching ratios).

hollow cathode emission current at a fixed E/N of 138 Td. The data presented in Fig. 4(a)–(c) demonstrate that the ion fragmentation pattern can be influenced by the conditions of the hollow cathode ion source. These figures show that the product ion branching ratios associated with the least exothermic channel corresponding to loss of H_2 becomes more significant above an emission current of 5 mA. In the case of 1-propanol, this channel was not observed at all when operating the hollow cathode at or below 5 mA. However, by 10 mA this channel has a branching ratio associated with it of approximately 5%. In the case of 2-propanol, the effect is even more dramatic; the ion branching ratio associated with that channel has substantially increased from approximately 1% when operating at below 5 mA to over 20% when operating at 10 mA. These observations suggest increasing hollow cathode emission current, which is achieved by increasing the voltage applied to the ion source, results in a higher effective temperature of the reagent ions. Fig. 4(a)–(c) also demonstrate that we did not exactly reproduce the branching ratios we obtained in the E/N studies at the fixed hollow cathode current of 5 mA. These differences may be attributed to the fact that after the E/N studies the hollow cathode source was cleaned (whereby carbon deposits were removed) which has also altered the ionising conditions. To illustrate that these changes are not associated only with the protonated water monomer, we repeated the measurements for cyclohexanol at an E/N of 92 Td, at which value the protonated water dimer is the most dominant reagent ion (see Fig. 1(a)). The results are presented in Fig. 4(d). At 92 Td three product ions are observed for cyclohexanol at m/z 83 (loss of water from the protonated monomer), m/z 99 (loss of H_2 from the protonated monomer) and m/z 81 (loss of H_2 from the protonated monomer followed by loss of H_2O), as found for the 138 Td study the m/z 99 channel shows a dramatic rise in branching ratio as the hollow cathode emission current is increased.

These experiments provide evidence that the internal energy distributions of the reagent ions are changing, which result in substantial changes in the probabilities associated with various reagent channels. Whilst this requires further investigations, it is clear that fragmentation patterns cannot be relied upon unless they are determined at exactly the same conditions when using the PTR-MS for monitoring purposes.

5. Conclusions

As observed in a recent study of unsaturated alcohols [14], within the drift tube environment of a PTR-MS the reactions of the reagent ions H_3O^+ with saturated alcohols proceed predominantly dissociatively. The product ion branching ratios are found to be very dependent on the value of the reduced electric field (E/N) used in the drift tube. Whilst this implies that E/N conditions must be provided in any PTR-MS study if comparisons of results are to be made between different investigations, this in itself may not be sufficient to ensure reproducible results. With a fixed E/N, differences will also arise between instruments because of variations in the conditions of the ionisation source. In this study we have undertaken some preliminary measurements relating to changes in the conditions for the production of the reagent ions, and presented some initial studies involving cyclohexanol, 1-propanol and 2-propanol. Changes in the product ion branching ratios are observed, which we have attributed to changes in the internal energy distribution within the reagent ions. An understanding and determination of the internal energy distribution of the reagent ions is therefore considered to be important if PTR-MS instrumentation is to be correctly characterised and to provide a fuller understanding of their operation. Further studies are therefore planned to investigate the internal energy distributions of the reagent ions in the drift cell of a PTR-MS.

In this paper we have highlighted that although PTR-(quadrupole) MS is an ideal instrument for monitoring (known) VOCs because of its extremely high sensitivity and fast response time, it can not be used to unambiguously assign a VOC to a given m/z (even when no fragmentation occurs) in a complex chemical environment. The potential complexity that may arise in interpreting PTR-MS spectra when dealing with complex chemical environments has however been reduced somewhat with the recent development of a high resolution PTR-TOF-MS to replace quadrupole mass spectrometric based instruments [23–25]. The high resolution available (up to $m/\Delta m$ 8000) is capable of distinguishing isobaric molecules (providing the mass separation is commensurate with the resolution, e.g., the instrument is easily capable of separating protonated formic acid at m/z 47.01 from protonated ethanol at m/z 47.05) and therefore allows the determination of the empirical chemical formula with a higher level of confidence than is achievable using a quadrupole mass spectrometer. However, even with the high resolution PTR-TOF-MS a m/z value is still insufficient to allow unambiguous identification of the VOCs present (even when an ion at the m/z value of the corresponding protonated parent is observed). Therefore, and as first mentioned by Lindinger et al. [3], other techniques, e.g., GC-PTR-MS may be required to (initially) aid in the identification. This is particularly true for those compounds that substantially fragment upon proton transfer from H_3O^+, as is the case for nearly all of the saturated alcohols investigated in this study.

Acknowledgements

References

[1] A. Hansel, A. Jordan, R. Holzinger, P. Prazeller, W. Vogel, W. Lindinger, Int. J. Mass Spectrom. Ion Process. 149/150 (1995) 609.
[2] Ionicon Analytik Ges.m.b.H. (see http://www.ptrms.com/).
[3] W. Lindinger, A. Hansel, A. Jordan, Int. J. Mass Spectrom. Ion Process. 173 (1998) 191.
[4] W. Lindinger, A. Hansel, A. Jordan, Chem. Soc. Rev. 27 (1998) 347.
[5] A. Hansel, A. Jordan, C. Warneke, R. Holzinger, A. Wisthaler, W. Lindinger, Plasma Sources Sci. Technol. 8 (1999) 332.
[6] C.N. Hewitt, S. Hayward, A. Tani, J. Environ. Monit. 5 (2003) 1.
[7] J.A. de Gouw, C. Warneke, Mass Spectrom. Rev. 26 (2007) 223.
[8] R.S. Blake, P.S. Monks, A.M. Ellis, Chem. Rev. 109 (2009) 861.
[9] C. Warneke, C. van der Veen, S. Luxembourg, J.A. de Gouw, A. Kok, Int. J. Mass Spectrom. 207 (2001) 167.
[10] A. Tani, S. Hayward, C.N. Hewitt, Int. J. Mass Spectrom. 223 (2003) 561.
[11] A. Tani, S. Hayward, A. Hansel, C.N. Hewitt, Int. J. Mass Spectrom. 239 (2004) 161.
[12] S. Kim, T. Karl, D. Helmig, R. Rasmussen, A. Guenther, Atmos. Meas. Technol. 2 (2009) 99.
[13] M. Demarcke, C. Amelynck, N. Schoon, F. Dhooghe, H. Van Langenhove, J. Dewulf, Int. J. Mass Spectrom. 279 (2009) 156.
[14] M. Demarcke, C. Amelynck, N. Schoon, F. Dhooghe, J. Rimetz-Planchon, H. Van Langenhove, J. Dewulf, Int. J. Mass Spectrom. 290 (2010) 14.
[15] J.A. Neuman, L.G. Huey, T.B. Ryerson, D.W. Fahey, Environ. Sci. Technol. 33 (1999) 1133.
[16] K. Buhr, S. van Ruth, C. Delahunty, Int. J. Mass Spectrom. 221 (2002) 1.
[17] J. de Gouw, C. Warneke, T. Karl, G. Eerdekens, C. van der Veen, R. Fall, Int. J. Mass Spectrom. 365 (2003) 223.
[18] R.S. Blake, K.P. Wyche, A.M. Ellis, P.S. Monks, Int. J. Mass Spectrom. 254 (2006) 85.
[19] S. Inomata, H. Tanimoto, Int. J. Mass Spectrom. 285 (2009) 95.
[20] A.J. Bell, K. Giles, S. Moody, P. Watts, Int. J. Mass Spectrom. Ion Process. 173 (1998) 65.
[21] A.J. Bell, K. Giles, S. Moody, N.J. Underwood, P. Watts, Int. J. Mass Spectrom. Ion Process. 165/166 (1997) 169.
[22] P. Watts, Anal. Proc. 28 (1991) 328.
[23] A. Jordan, S. Haidacher, G. Hanel, E. Hartungen, L. Märk, H. Seehauser, R. Schottkowsky, P. Sulzer, T.D. Märk, Int. J. Mass Spectrom. 286 (2009) 122.
[24] F. Petersson, P. Sulzer, C.A. Mayhew, P. Watts, A. Jordan, L. Märk, T.D. Märk, Rapid Commun. Mass Spectrom. 23 (2009) 3875.
[25] C.A. Mayhew, P. Sulzer, F. Petersson, S. Haidacher, A. Jordan, L. Märk, P. Watts, T.D. Märk, Int. J. Mass Spectrom. 289 (2010) 58.